J Mater Sci (2006) 41:8166–8172
DOI 10.1007/s10853-006-0392-1

Electronic transport in dielectrophoretically grown nanowires

C. T. Harrower · D. R. Oliver

Received: 31 December 2005 / Accepted: 1 May 2006 / Published online: 28 October 2006

Abstract Gold nanoparticles with mean diameter 10–15 nm have been synthesized and stabilized using capping agents in a polar solvent (water) and a non-polar solvent (dodecane). Using two gold bond wires (diameter 0.25 mm and separated by less than 10 μm) as electrodes a sinusoidal driving voltage was applied to the solution. The resulting dielectrophoresis of the solution caused deposition of these nanoparticles at the electrodes and the formation of a wire between the electrodes. Conductance studies of the wire as the final connection formed yielded evidence for low-dimensional transport character in the form of discrete (Landauer) conductance steps. Histogram analysis of the conductance data further supports the conclusion that as the wire forms the capping agents do not always contribute to the electronic transport through the wire.

Introduction

It may be postulated and demonstrated that an individual molecule can, in appropriate conditions, exhibit electrical transport character similar that exhibited by diodes, resistors or even transistors. How electrical 'connections' are made to a molecule, let alone demonstration of the existence and/or reliability of such a connection, remains the subject of vigourous debates [1–4]. At the core of these discussions remains a basic concern over whether or not the electrical character is largely, even entirely, due to whatever connection exists. Physically attaching a molecule to a metallic surface is but one of the challenges which include having a metallic surface that is so small that only one molecule attaches to it, or having adequately dispersed molecules at the interface that their individual connections and associated contributions may be studied.

The goal of this study is to align a 'chain' or wire of gold nanoparticles between macroscopic contacts and to study the conduction character of this chain. In principle, the contact points between individual nanoparticles are small and have limited dimensionality, thus the system may provide a good template for contact behaviour in molecular electronics. The creation of this wire of gold particles may be achieved through dielectrophoresis of a colloidal suspension between two electrodes.

Materials, syntheses and experimental procedures

Materials

The materials used in this study were obtained from commercial vendors and used as received unless dissolved in sufficient de-ionized (DI) water to obtain the concentrations specified. The precursor for the nanoparticle synthesis was tetrachloroaurate(III) trihydrate ($HAuCl_4 \cdot 3H_2O$) as purchased from Acros Organics BVBA, or hydrogen tetrachloroaurate(III) solution ca. 30 wt% solution in dilute HCl (99.99%) as

C. T. Harrower · D. R. Oliver (✉)
Electrical & Computer Engineering, University of Manitoba, E3-390, EITC, 75a Chancellor's Circle, Winnipeg, MB, Canada, R3T 5V6
e-mail: derek@ee.umanitoba.ca

purchased from Sigma-Aldrich. The choice of precursor did not result in any discernable difference in nanoparticle yield or size distribution. For the other reagents, poly(*N*-vinyl-2-pyrrolidone) (PVP) was purchased from Matheson Coleman and Bell, sodium citrate, 2-propanol, potassium bitartrate, and octadecanthiol (ODT) were purchased from Fisher Scientific. Glassware used was scrupulously cleaned with *aqua regia* and rinsed three times using DI water.

Syntheses

The colloidal gold was synthesized through the reduction of tetrachloroauric acid in solution by a reducing agent in the presence of a stabilizing ligand (capping agent). In each case the role of the capping agent was to arrest aggregation of the nanoparticles as the synthesis proceeded, thus enabling some control over the particle size distribution.

Citrate-capped gold nanoparticles were produced following the method outlined by Frens [5], a method that has been developed and rigorously studied by later authors [6–8]. 50 ml of aqueous 23 mM tetrachloroaurate(III) solution was heated to 100 °C and 1 ml of 1 wt% sodium citrate was added to the hot solution while stirring vigorously. Within 2 min the solution changed colour from pale yellow to orange-red indicating nanoparticle formation. After a further 5 min stirring (to ensure completion of the reaction) the solution was concentrated in a rotary evaporator operating at 40 °C.

Poly(N-vinyl-2-pyrrolidone)-capped gold nanoparticles were produced following a method similar to that outlined by Tan et al. [9]. Twenty millilitre of 1 mM aqueous tetrachloroaurate(III) solution containing 1.6 g of PVP was brought a boil. 20 ml of 0.5 wt% potassium bitartrate that had separately been heated to 100 °C, was added quickly while stirring vigorously. After 2 min the solution colour changed from yellow to a deep red (similar to the colour of red wine) indicating nanoparticle formation. After stirring for another 5 min, to ensure completion of the reaction, the solution was completely dried in a rotary evaporator operating at 40 °C. The resulting deposit was then re-dissolved in 1-propanol, chosen as potassium bitartrate is negligibly soluble in 1-propanol. After separation from the potassium bitartrate residue, the 1-propanol solution was used as a host solution for the colloidal particles, or it was dried once more in the rotary evaporator and the nanoparticles re-dissolved in DI water to form an aqueous colloidal suspension.

Octadecanthiol-capped gold nanoparticles were synthesized using a process based on those reported by Carotenuto and Nicolais [10] with reference to the initial work of Brust et al. [11]. Initially, 30 ml of 30 mM aqueous tetrachloroaurate(III) solution was mixed with 2.19 g of tetraoctylammonium bromide in 80 ml of toluene. The mixture was stirred vigorously to ensure that the two immiscible phases were well-mixed. Once mixed, 240 mg of ODT and 25 ml of 0.4 M aqueous sodium borohydride were added. This caused a colour change from off-white (milky) to brown. To ensure completion of the reaction, the phases were stirred continuously for a further 3 h, when the toluene phase was separated and concentrated to ~10 ml in a rotary evaporator operating at 70 °C. The remaining solution was allowed to return to room temperature, at which point 400 ml of ethanol was added. This dissolved excess ODT and tetraoctylammonium bromide as well as dispersing the nanoparticles which formed a brown precipitate. The ethanol/nanoparticle solution was stored overnight in the dark at –18 °C during which time the precipitated (but still-capped) nanoparticles aggregated to the extent that they could be separated by filtration. Following the completion of this step, the nanoparticles were re-dissolved in dodecane or toluene as required. This re-dissolution reversed the aggregation that had occurred in the presence of ethanol, i.e., yielding nanoparticles on the order of 10 nm in diameter [9–13].

It is an interesting historical footnote that Faraday's 1857 Bakerian Lecture [14] not only contains one of the first documentations of the characteristic colour of colloidal solutions but also outlines a two-phase synthesis pathway for obtaining these solutions that is remarkably similar to that described above for the ODT synthesis.

Experimental procedures

As described previously [15], the size distribution of the nanoparticles synthesized was obtained from transmission electron microscope (TEM) images of samples dried onto a TEM grid (Marivac Inc.: (185, 400 mesh carbon coated copper grid). The size distributions were obtained using an algorithm based upon the circular Hough transform [16, 17] implemented in MATLAB. This approach was found [15] to be more reliable and robust than calculations based on Mie theory [18, 19]. It should be noted that the number of washing and re-dissolution steps did not change the nanoparticle size distributions determined in this manner. For all the systems described above, the mean diameter of the nanoparticles was found to be in the range 10–15 nm.

Mechanical break junction experiments have been used to study the electronic transport characteristics of nanometre-scale metallic contacts. These experiments have involved bringing macroscopic electrodes into and out of contact using a mechanical stage. Incremental steps observed in the conductance (I–V character) of the formed junction have been attributed to the formation of a nanometre-scale conduction path at the junction. These non-linear conductance 'steps' have been reported at integer values of $2e^2/h$ (G_0), a quantity derived from the density of states available to the charge carriers [20–29]. In a such one-dimensional system, the density of states can appear to have no energy-dependence and charge carriers passing through this region do so without experiencing any scattering, hence the apparent absence of normal (metallic) conduction character regardless of the ambient temperature.

To provide some basis for comparison when fabricating the metallic contact via dielectrophoresis, mechanical break junction experiments in which two freshly cut gold wires (diameter 0.25 mm) were slowly brought into contact and separated using the micrometer drive. Throughout, a sinusoidal signal of $V = 0.1 + 0.05\cos(10\pi t)$, was applied to the junction and conductance determined from the data. These mechanical break junction experiments were performed in air, DI water, dodecane and solutions of the capping agents and the raw conductance data indicate some evidence [15] for the conductance steps at integer values of G_0 referred to above.

Dielectrophoretically grown wires were obtained using the apparatus illustrated in Fig. 1. Two freshly cut gold wires (diameter 0.25 mm) were manually brought into contact then separated by less than 10 μm using the micrometer drive and an optical microscope. An applied voltage, $V_d = 0.2 + 0.5\cos(10\pi t)$, was used to encourage dielectrophoretic motion of the gold nanoparticles towards the electrodes and, in turn, wire formation. As a wire formed, the current through the junction increased significantly, triggering the comparator which in turn switched the driving voltage to a lower amplitude, V_d–$V_H = 0.02 + 0.05\cos(10\pi t)$, slowing the wire growth and enabling the conductance at the junction to be monitored.

All experiments were conducted at room temperature with the apparatus set up on a vibration isolation table. Care was taken to minimize acoustic noise, but the experimental apparatus was not completely isolated from external noise of this nature. The present study has been conducted without the use electron-beam lithography to fabricate the electrodes nor a low temperature (4.2 K) environment for the I–V measurements.

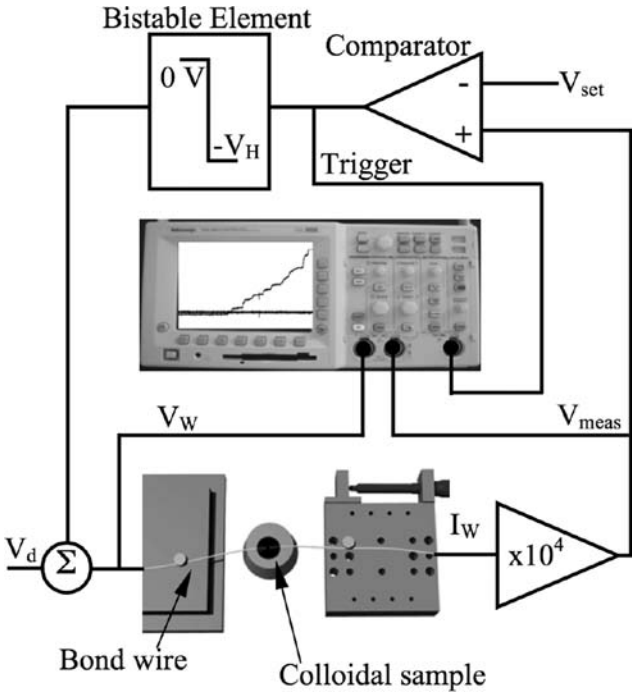

Fig. 1 Diagram of the apparatus used for the dielectrophoretic growth of the nanowires. The current driven between the electrodes was converted to a voltage by a low-noise transresistance amplifier

Results

Plots of raw conductance, as integer values of G_0, can give some indication that low-dimensional conductance has occurred at the junctions whether these are obtained through mechanical means or via dielectrophoretic growth. Figure 2 shows four such plots; controls in the form of mechanical break junction data (Fig. 2a–b) and data from dielectrophoretically grown wires as the wire forms (Fig. 3a–b). The time taken to form a wire via dielectrophoresis of the colloidal solution ranged from a few minutes to about 20 min. The initial electrode spacing was manually achieved and therefore contributed significantly to this range. Once formed, the wire could be held in an apparently low-dimensional state for between half a minute and about 2 min depending on the ongoing rate of aggregation. Wires, once formed, have been manually broken using the micrometre drive and then re-formed dielectrophoretically. However the re-formed wires did not retain their low-dimensional state as long as they would on initial formation.

Additional experiments using large copper electrodes separated by 0.2 mm, fashioned from a copper-coated dielectric substrate with a milling machine, were undertaken with a view to resolving the reproducibility

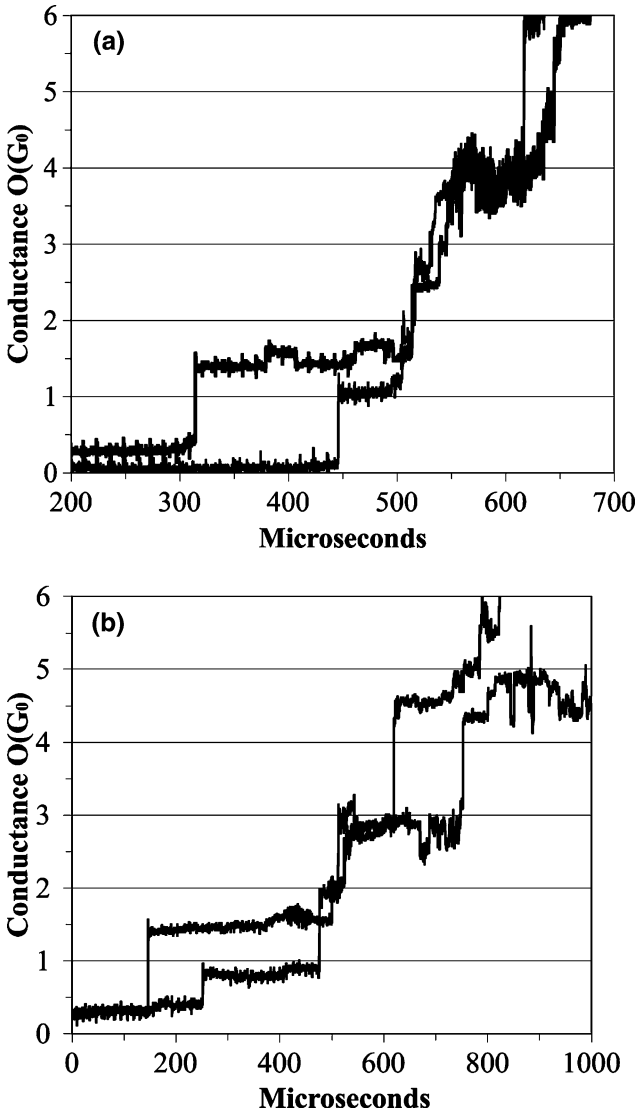

Fig. 2 Conductance data obtained from mechanical 'make' junction experiments conducted as the electrodes were manually brought closer together in (**a**) aqueous PVP and (**b**) ODT dissolved in dodecane. The driving voltage for these experiments was $0.15\sin(10\pi t)$ V

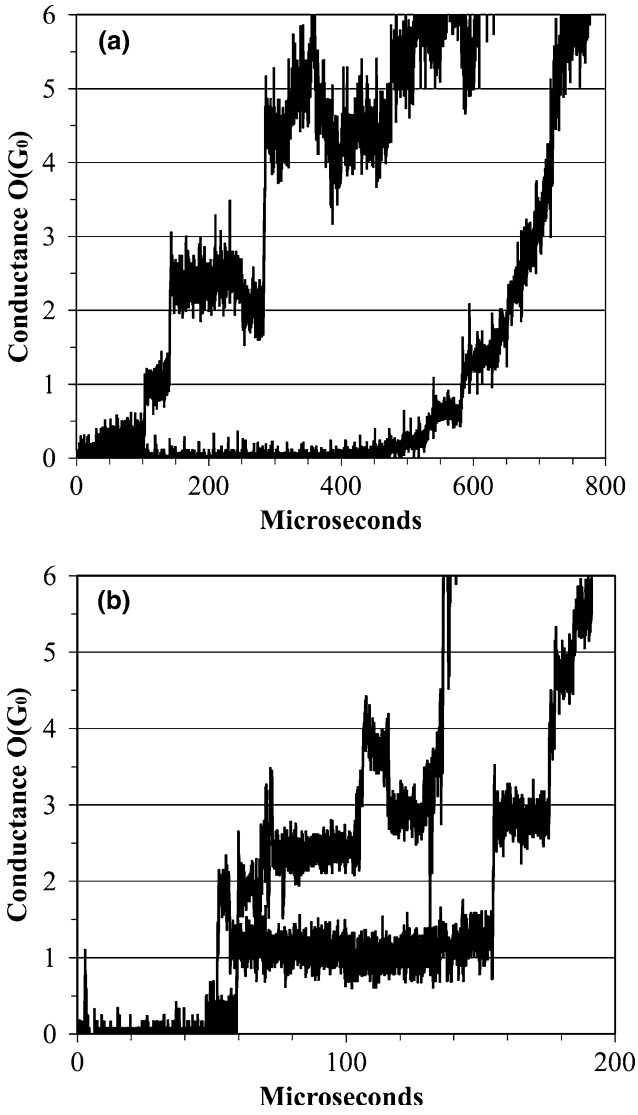

Fig. 3 Conductance data obtained from dielectrophoretic growth experiments as the wire formed from gold nanoparticles stabilized with (**a**) PVP and (**b**) ODT. The PVP-capped nanoparticles were suspended in water. The ODT-capped nanoparticles were suspended in dodecane

issue of electrode spacing. The greater separation of these electrodes (~10× that discussed above) and the electrode size meant that the wire formation process was less efficient. The wires formed were on the order of microns thick, i.e. visible with an optical microscope, and similar to those reported by Velev et al. [30, 31]. This reflected similarities in electrode sizes and spacing between these two experiments.

The data presented in Figs. 2 and 3 indicates some stability and therefore possibly quantization of conductance in the junctions at integer values of $2e^2/h$ (G_0). However these data are far from conclusive and many workers in this field prefer to use histograms compiled from many conductance traces in order to determine whether the apparent plateaus in conductance are statistically significant—an example of such work involving metallic and molecular junctions treated in this fashion may be found in [32]. While histograms may not constitute absolute proof of conductance quantization [33–35], they do provide a useful reference frame in which to evaluate the significance of the data obtained. The histograms presented in Figs. 4 and 5 were compiled from over 30 experiments such as those represented in Figs. 2 and 3. Worst-case measurement errors were used to determine the ranges into which the raw data were 'binned'.

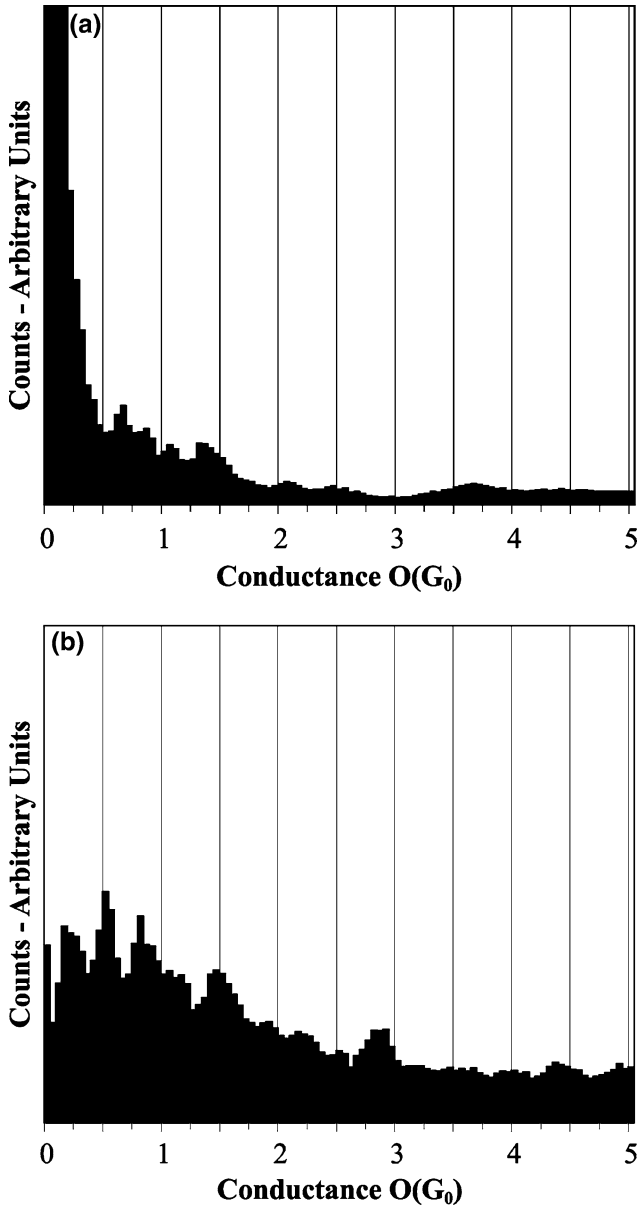

Fig. 4 Histograms obtained from over 30 sets of mechanical break junction conductance data such as that shown in Fig. 2: (**a**) aqueous PVP and (**b**) ODT dissolved in dodecane

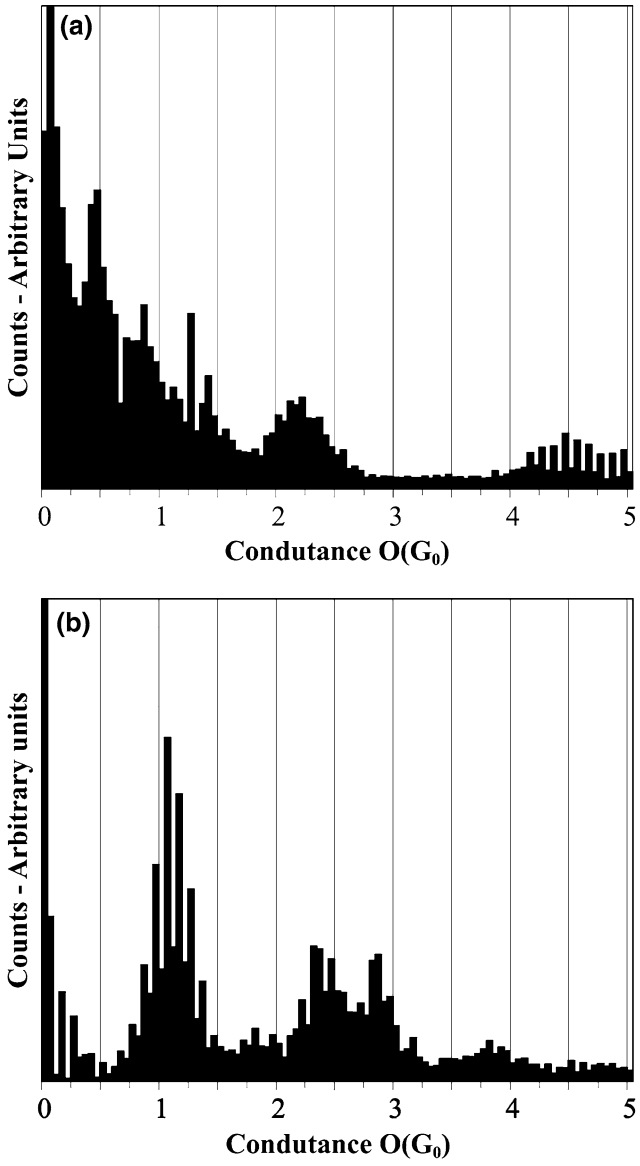

Fig. 5 Histograms obtained from over 30 sets of dielectrophoretically grown wire conductance data such as that shown in Fig. 3: (**a**) PVP-capped nanoparticles suspended in water, (**b**) ODT-capped nanoparticles suspended in dodecane

While the mechanical break junction data appear inconclusive, the wires grown dielectrophoretically from ODT-capped nanoparticles in dodecane do appear to exhibit quantized conductance at integer values of $2e^2/h$ (G_0).

Wire growth was undertaken at a variety of temperatures well above room temperature (by placing the apparatus on a heating mantle). These experiments helped confirm the observation that the principle sources of noise in the experimental signals were due to the electronics surrounding the electrodes and the solution and that the results obtained were not affected by the temperature at which the experiment was conducted.

Discussion

In the forgoing it has been assumed that the electronic 'pathway' between the external connections of the system is through gold, whether during a mechanical break junction experiment or following dielectrophoresis. In essence, the (realistic possibility) of the capping agents forming part of this conduction

pathway has been neglected. The histograms in Figs. 4 and 5 provide a clear reminder of the importance of the capping agents to the electronic interaction.

For the PVP 'control' histogram (Fig. 4a) looks more like an exponential decay with increasing conductance—characteristic of tunnelling contributions to the conductance that are frequently associated with transport through the intervening solution and/or the capping agents. However, there is some evidence for peaks at integer values of G_0 in the ODT control histogram (Fig. 4b). Dielectrophoretic growth with PVP-capped nanoparticles (Fig. 5a) appears to strengthen the histogram peaks near G_0 and $2G_0$, although the strong peak at 0.5 G_0 and the remnant signal close to zero conductance indicate that while some low-dimensional influence may be present, the data presently available do not strongly support the hypothesis that a dielectrophoretically grown wire yields a nanoscale junction as it forms. With only ~30 repetitions of the experiment, these data are at the fringes of statistical significance; this 'null' result might be misleading if a greater volume of data were to be analyzed.

The histograms obtained from ODT solutions/nanoparticles yield a far more encouraging result. Neither histogram (Figs. 4b or 5b) suffers from the large contribution close to zero conductance as seen in the PVP data. While there is mixed evidence for clear peaks in the control histogram (Fig. 4b), the peak at G_0 in Fig. 5b is not only clearly defined but substantially different from the control histogram (Fig. 4b).

Imperfections in the contacts used for these experiments may contribute to some of the anomalies mentioned above. A number of investigations [36–39] have sought to attribute fractional values of G_0 to impurities (stoichiometric or crystalline) in the contacts. The contacts (bond wires) used in this investigation would be prone to exhibiting most of these imperfections. Equally, the influence of the capping agents cannot be ignored. A lengthy and investigation into the location, 'adherence' and electronic character of any capping agent could be undertaken. However, for a system to exhibit ballistic conduction through a molecular connection, the accessible electronic states in the molecule must be well-aligned with similar states in the metal contact, i.e., the likelihood of such is incredibly small. Indeed, it is reasonable to argue that obtaining the signature of low-dimensional (ballistic) transport in this system implies a metallic link through a chain of partially fused nanoparticles that have aggregated from solution onto the electrodes.

Similar experiments to those discussed above have been undertaken with citrate-capped nanoparticles. However the number of experiments have been completed to date is insufficient to justify representation of these data in histogram form.

Conclusions

Gold nanowires have been grown via dielectrophoresis of a variety of colloidal gold solutions. As they form these wires appear to exhibit discrete steps in conductance that match those predicted by Landauer theory. Histogram analysis of the conductance traces leads to the conclusion that wire growth from ODT-capped gold nanoparticles does yield a nanoscale metallic wire at the point of formation, while for PVP-capped nanoparticles it appears that there are other contributions to the conductance. The precise influence of the capping agents may be ignored if the evidence for low-dimensional conductance steps is strong, as in the ODT case. It is possible to hold the wires in the low-dimensional conductance state for a few minutes, although improvements to the feasibility of this step are the subject of ongoing investigations.

Acknowledgements The authors are grateful for access to the microscopy facilities in the Department of Mechanical & Industrial Engineering at the University of Manitoba as well as access to equipment and reagents in the laboratories of, as well as advice and encouragement from Dr. T. Hegmann and Dr. S. Kroeker in the Department of Chemistry, University of Manitoba. The work reported has been undertaken in facilities provided with assistance from the Canadian Foundation for Innovation (CFI), the Provincial Government of Manitoba and Western Economic Diversification Canada (WD). The project has been funded by grants from the Natural Sciences and Engineering Research Council of Canada (NSERC) and the University of Manitoba. DRO acknowledges support from the Canadian Institute for Advanced Research (CIAR) Nanoelectronics Initiative.

References

1. Reed MA, Zhou C, Muller CJ, Burgin TP, Tour JM (1997) Science 278:252
2. Emberly EG, Kirczenow G (2001) Phys Rev B 64:125318
3. Emberly EG, Kirczenow G (2001) Phys Rev B 64:235412
4. Mantooth BA, Weiss PS (2003) Proc IEEE 91:1785
5. Frens G (1973) Nature 241:20
6. Slot JW, Geuze HJ (1981) J Cell Biol 90:533
7. Geuze HJ, Slot JW (1985) Eur J Cell Biol 38:87
8. Lin Y, Ge-Bo P, Su GJ, Fang X, Wan L, Bai C (2003) Langmuir 19:10000
9. Tan YW, Dai XH, Li YF, Zhu DB (2003) J Mater Chem 13:1069
10. Carotenuto G, Nicolais L (2003) J Mater Chem 13:1038
11. Brust M, Walker M, Bethell D, Schriffrin DJ, Whyman R (1994) J Chem Soc Chem Commun 15:801
12. Sarathy KV, Raina G, Yadav GU, Kulkarni GU, Rao CNR (1997) J Phys Chem B 101:9876

13. Kim DH, Noh J, Hara M, Lee H (2001) B Kor Chem Soc 22:276
14. Faraday M (1857) Philos Trans Roy Soc London 147:145
15. Oliver DR, Harrower CT (2006) Key Eng Mat 314:121
16. Ritter GX, Wilson JN (1996) In: Handbook of computer vision algorithms in image algebra, CRC Press, Boca Raton, Florida, USA, p. 246
17. Yla-Jaaski A, Kirati N (1992) IEEE Trans Pattern Anal Machine Intell 14:496
18. Mie G (1908) Annalen der Physik 25:377
19. Huang S, Minami K, Sakaue H, Shingubara S, Takahagi T (2002) J Appl Phys 92:7486
20. Landauer R (1957) IBM J Res Dev 1:223
21. Landauer R (1970) Philos Mag 21:863
22. Ott F, Lunney J (1998) Europhys News 13
23. Todorov TD, Sutton AP (1996) Phys Rev B 54:14234
24. Skorodumova NV, Simak SI (2003) Phys Rev B 67:121404(R)
25. da Silva EZ, da Silva AJR, Fazzio A (2001) Phys Rev Lett 87:256102
26. Li CZ, Sha H, Tao NJ (1998) Phys Rev B 58:6775
27. Tekman E, Ciraci S (1991) Phys Rev B 43:7145
28. Okamoto M, Takayanagi K (1999) Phys Rev B 60:7808
29. Agraït N, Yeyati AL, van Ruitenbeek JM (2003) Phys Rep 377:81
30. Hermanson KD, Lumsdon SO, Williams JP, Kaler EW, Velev OD (2001) Science 294:1082
31. Bhatt KH, Velev OD (2004) Langmuir 20:467
32. Xu B, Tao NJ (2003) Science 301:1221
33. Scheer E, Joyez P, Esteve D, Urbina C, Devoret MH (1997) Phys Rev Lett 78:3535
34. Yanson AI, Van Ruitenbeek JM (1997) Phys Rev Lett 79:2157
35. Dreher M, Pauley F, Heurich J, Cuevas JC, Scheer E, Nielaba P (2005) Phys Rev B 72:075435
36. de Heer WA, Frank S, Ugarte D (1997) Z Phys B 104:469
37. García-Martín A, del Valle M, Sáenz JJ, Costa-Krämer JL, Serena PA (2000) Phys Rev B 62:11139
38. Csonka S, Halbritter A, Mihály G, Jurdik E, Shklyarevskii OI, Speller S, van Kempen H (2003) Phys Rev Lett 90:116803
39. Itakura K, Yuki K, Kurokawa S, Yasuda H, Sakai A (1999) Phys Rev B 60:11163